Physiological signal processing for affective state estimation during a Human-Robot Interaction

William Hoiles George Sterling Susana Zoghbi

***Abstract*— Being able to estimate people's affective states when interacting with a robot is essential for developing a safe environment where humans and robots work together. In particular, robots need to be able to sense humans around them, identify human reactions and respond accordingly. Physiological signals can be used for this purpose. The aim of this project is to implement wavelet shrinkage techniques on electrocardiogram, electromyogram and skin conductance signals -measured during a human-robot interaction task- in order to identify relevant features for the estimation of human affective states.**

I. INTRODUCTION

Robots have been successfully employed in industrial settings to improve productivity and perform dangerous or monotonous tasks. However, there is an increasing need for robots to perform home-care/daily tasks to assist people in office or home settings. Enhancing robot capabilities would allow seniors and people with physical impairments to independently enjoy a high quality of life. To achieve this goal, it is essential that robots interact with people in a safe and friendly manner. Thus, robots need to be able to sense humans around them, identify the degree of comfort towards the robot's motions, and respond accordingly during an interaction. For example, if certain robot motions produce discomfort due to high speed or proximity, the robot should be able to identify the elicited affective state and respond accordingly by slowing down and/or maintaining a larger distance.

In order to identify human affective states, we propose the use of physiological signals, i.e. electrocardiography (ECG), electromyography (EMG) and skin conductance rate (SCR). The purpose of this project is to implement wavelet shrinkage techniques to identify relevant features from biosignals. The extracted features are used to train a Neural Network to estimate affective states reported by users during a human-robot interaction.

A. Affective-State Representation

A two-dimensional map is used to represent human affective states as valence and arousal [1]. This space can be thought of as a Cartesian space with valence on the x-axis and arousal on the y-axis, as shown in Figure 1. Valence measures the degree to which the emotion is positive or negative, and arousal measures the strength of the emotion. This representation system has been favored for use with physiological signals and in psychophysiological research [1].

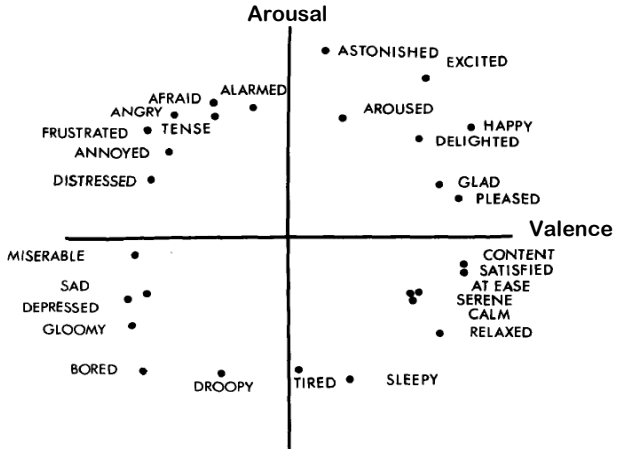

Figure 1 – Affective State Cartesian space representation [1].

B. *Reporting Affective States*

A hand-held device was employed to allow the user to report emotions while interacting with the robot. The handheld device has two inputs, as shown in Figure 2. By using the forward/backward motion, the indication of valence is registered. The forward motion relates to positive mood and the backward motion to negative mood. By squeezing the handle, the level of intensity of this mood is recorded where no squeezing represents low intensity and forceful squeezing represents high intensity.

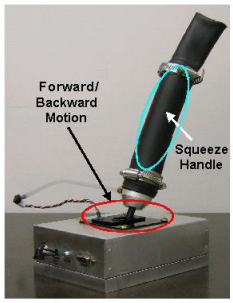

Figure 2 – On-line Affective State reporting device

C. *Data collection*

Physiological signals were collected during a human-robot interaction experiment using the Procomp Infinity biosensors system from Thought Technology [2]. All sensor data were collected at 256 Hz. During the experiment, the human subject was seated facing the robot. The robot was initially held motionless for a minimum of 90 s to collect baseline physiological data for each subject. The robot then executed the 7 different motions while the participant reported his affective state using the hand-held device.

D. *Signal processing using Wavelets*

This section introduces the rational for using wavelets and presents a brief description of its theory.

Rational for using Wavelets - The Wavelet Transform has been shown to be a very good tool for local analysis of non-stationary and fast transient signals [12]. It is able to do this because it does both time and frequency localizations [12]. The Short Time Fourier Transform (STFT) can be used to analyze non-stationary signals, but the STFT gives a constant resolution at all frequencies, the WT uses multi-resolution technique by which different frequencies are analyzed with different resolutions [12]. The noise may be associated with the same frequency as the desired signal [13]. This means that we cannot use a regular frequency filter because would induce noticeable loss of information of the desired signal [12].

Theory - The DWT is used to translate data from the time domain to the wavelet domain [3]. The wavelet transformation decomposes a signal f(t) into a linear decomposition of sums, where f(t) is the products of the wavelet coefficients and the wavelet functions [3]. Roughly the localization in time is done with k and localization in frequency is done with j [3].

$$f(t) = \sum_{k=0}^{2^{j_0}-1} a_{j_0 k}\, \phi_{j_0 k}(t) + \sum_{j=j_0}^{J} \sum_{k=0}^{2^j-1} d_{jk}\, \psi_{jk}(t)$$

The coefficients "*d*" are the details and the coefficients "*a*" are the approximations [13]. An overview of Mallat's cascade algorithm was used to describe how to find the coefficients of the shift invariant DWT (SWT) [3] The mother wavelet and father wavelets are shown below where j indicated the level of decomposition and k represents the translations of the wavelet [13].

$$\psi_{jk}(t) = 2^{j/2}\psi(2^j t - k)$$
$$\phi_{jk}(t) = 2^{j/2}\phi(2^j t - k)$$

Since the space of $\psi(2(t-k))$ contains the space of $\psi(t)$ it is possible to represent $\psi(t)$ as a linear combination of functions from the space of $\psi(2(t-k))$ [3] An equivalent relation can be made between $\phi(2(t-k))$ and $\phi(t)$ [3]. Using this result we obtain the relations

$$\phi(t) = \sum_{k\epsilon\mathbb{Z}} h_k\sqrt{2}\phi(2x-k)$$
$$\psi(t) = \sum_{k\epsilon\mathbb{Z}} g_k\sqrt{2}\phi(2x-k)$$

Where **h** is a low-pass filter and **g** is a high-pass filter [3]. We then successively convolve the signal with the filters $h^{[r]}$ and $g^{[r]}$ to obtain the wavelet coefficients [3]. In order to make the wavelet decomposition stationary the filters must be up sampled such that every filter $h^{[r]}$ and $g^{[r]}$ is obtained by inserting zeros between the taps in $h^{[r-1]}$ and $g^{[r-1]}$ [3] The decomposition process is shown below.

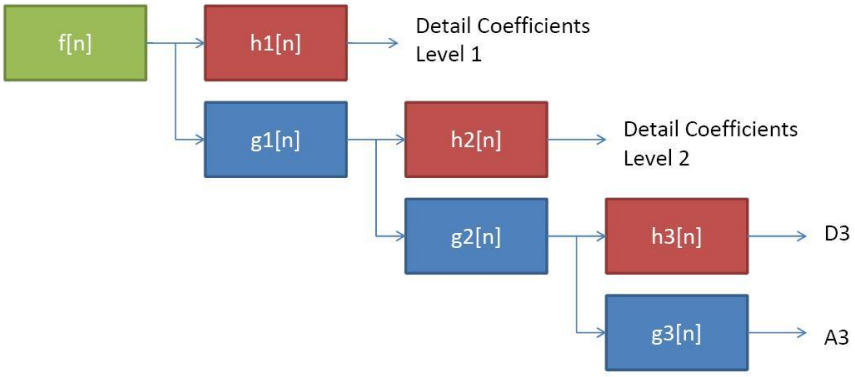

Figure 3 – Wavelet decomposition process

The results of the SWT decomposition are a set of detail coefficients representing high frequency components, and one single set of approximation coefficients representing the low frequency content of the signal [13].

II. Methodology

A. Physiological signal Processing using Wavelets

Choice of Wavelet - There are no set rules for the choice of wavelet to be used [14]. Ideally the wavelet decomposition being used would produce a small number of large coefficients related to the desired signal, and the rest would be small coefficients related to noise [13]. When a desired signal is mixed with noise then the noise is spread over all coefficient levels, normally the first detail level contains the most noise [15]. It can then be assumed the small coefficients are harder influenced by noise [13]. A variety of shift invariant wavelets were analysed using MATLAB to determine which would be well suited for decomposing the ECG, SCR, and EMG signals. From this analysis the best results were obtained using the Daubechies wavelets; thus, we will analyse the family of Daubechies wavelet family for decomposing the noisy ECG, SCR, and EMG signals.

Denoising Using Shrinkage - The noise present in a signal can be removed by applying a wavelet shrinkage denoising method which will preserve the desired signal characteristics, regardless of the frequency content it contains [15]. Wavelet shrinkage is done by modifying the wavelets coefficients in a way such that the "small" coefficients associated to the noise are neglected [15]. The signal can then be reconstructed from these filtered coefficients to produce a clean signal [15]. There are various methods that have been developed for wavelet shrinkage, the most common use coefficient thresholding. The denoising methods differ in their choice threshold λ and the thresholding filter that determines how the threshold is applied [15]. The thresholding filters that will be examined are the Hard-Thresholding, and Soft-Thresholding filters [15]. The thresholding rules that will be examined with the thresholding filters are Universal Threshold using a standard estimator and median absolute deviation from median (MAD) for the standard deviaton, SureShrink, Cross Validation, and Block Thresholding [3].

Electromyography (EMG):

The EMG is the primary source of information for muscle movement [7]. EMG signals are generally affected by hardware for signal amplification and digitization, movement of cables during data collection and the activity of the motor units distant from the detection point [5]. The main problem in recording EMG signals is that several muscle activities occur simultaneously that are all recorded by the electrode attached to the skin [6]. In this study the detection of the occipito-frontalis muscle activity is being performed using an EMG that is placed in the center of the forehead. The activation of this muscle group will show if the patient is frowning or not.

Synthetic EMG Model:

The development of a synthetic EMG was done using the exponentially modified Gaussian function (EMGF) constructed from [4]. In order to create a realistic signal the parameters for each EMGF are chosen to resemble the waveforms present in the real EMG signals. There are 4 main parameters that need to be determined in order to construct the EMGF [4]. These parameters are amplitude, retention time of the peak, standard deviation of the Gaussian peak, and decay rate of the EMGF [4]. In this study a serious of EMGFs are superimposed on each other in order to create a synthetic EMG that is similar to the real EMG signals. Gaussian noise is added to the superimposed EMGFs to simulate the noise present in the real EMG signals. A comparison of the real EMG and synthetic EMG can be made in Figure 4.

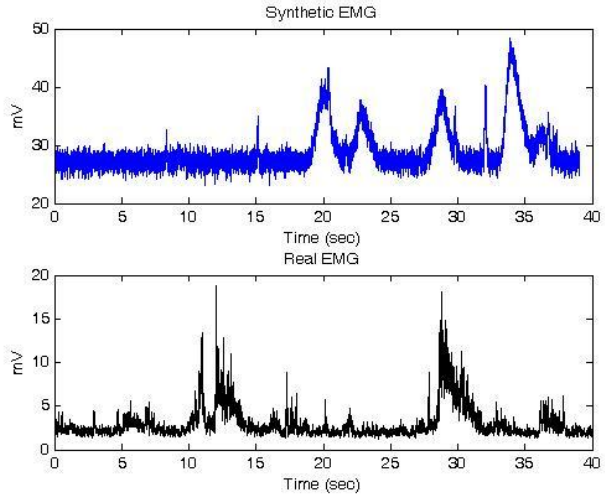

Figure 4 – Comparison between real EMG (bottom) and synthetic EMG (top)

Filtering Method:
Applying SWT using Daubechies-1 wavelets with a 7-level decomposition using the SureShrink method produced the best results out of the Daubechies family when compared with the other methods. A RMSE table was produced in Appendix A showing the RMSE value for each threshold filter and rule combination. The desired signal characteristics are obtained by reconstruction of the using only the sixth and seventh filtered detail coefficient levels with the approximation details. The results of applying this algorithm can be seen in Figure 5. As well from visual inspection between the different shrinkage methods this combination performs the best for the real EMG signals.

Detecting Muscle Activation:
In order to detect the activation of the occipito-frontalis muscle from the EMG a single-threshold method will be used on the filtered EMG signal [8]. The amplitude of the threshold is based on the mean and standard deviation of the signal [8]. In the thresholding routine any bursts that are separated by less than 125ms are joined together, while any burst clusters that are less than 50ms are eliminated [8]. Figure 5 provides a graphical representation of the thresholding method to determine muscle activation from the synthetic EMG in Figure 4.

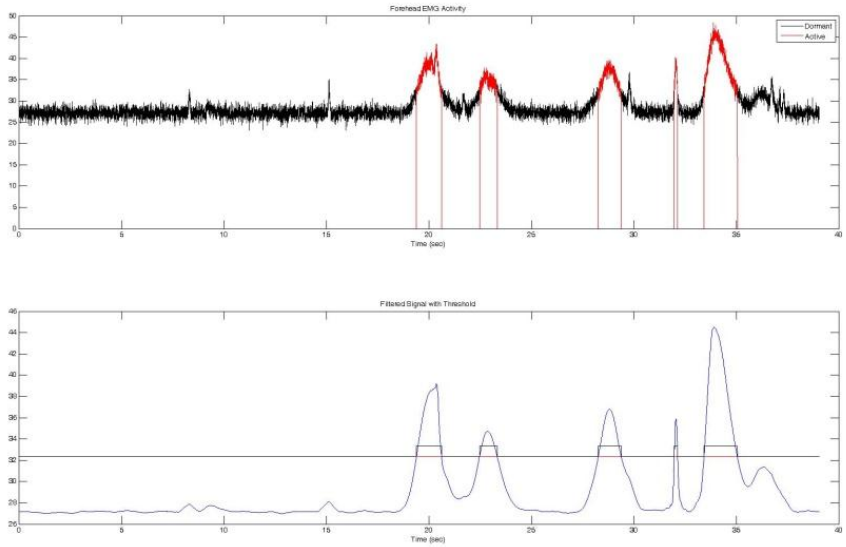

Figure 5 – Graphical representation of thresholding method for filtered EMG

ECG:
The ECG is a time varying signal that is used to represent the ionic current flow which causes the cardiac fibers to contract and subsequently relax [9]. A single normal cycle of the ECG represents the successive atrial depolarization/repolarization and ventricular depolarization/repolariztation which occurs with every heartbeat [9]. The recording environment introduces noise such as spurious signals from nearby equipment, poor electrodes, electromagnetic pollution, and physiological processes which are not related to the heartbeat which are superimposed on the ECG [10].

Synthetic ECG:
The production of a synthetic ECG was done using the method purposed in [9]. The parameters in the model are varied to resemble the real ECG data. The addition of Guassian noise is done to simulate the noise present in the real ECG signal. The real and synthetic ECG signals can be viewed in Figure 6.

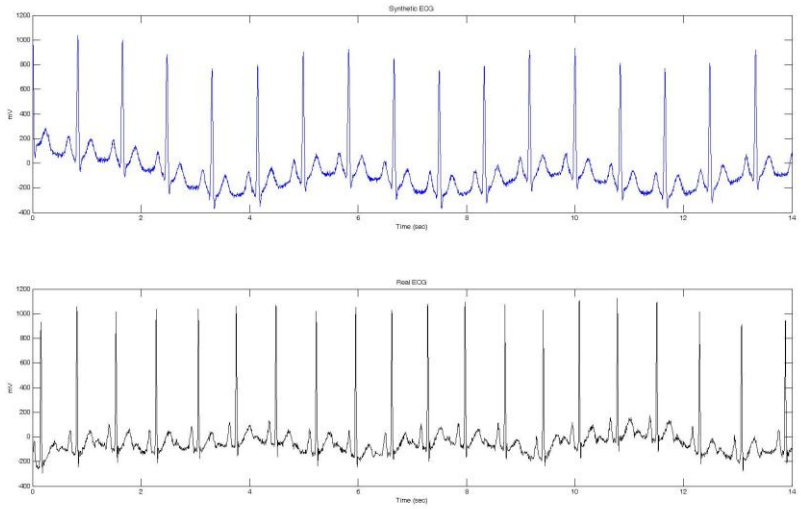

Figure 6 – Real (bottom) and synthetic ECG (top) signals

Filtering Method:

The application of the Daubechies-8 wavelets with a 4-level decomposition using the Universal Threshold with the standard deviation calculated using the MAD method. This was chosen because with the analysis of the synthetic ECG and filtering routing the lowest RMSE was obtained using this set of parameters. As well the last approximation details and first detail coefficients are set to zero because they do not contain any significant details for the extraction of the clean ECG. A figure of the un-filtered details and approximation details can be seen in Figure 7 where it is evident that the first detail level is saturated with noise. The result of applying this filter to a noisy ECG signal can be viewed in Figure 8.

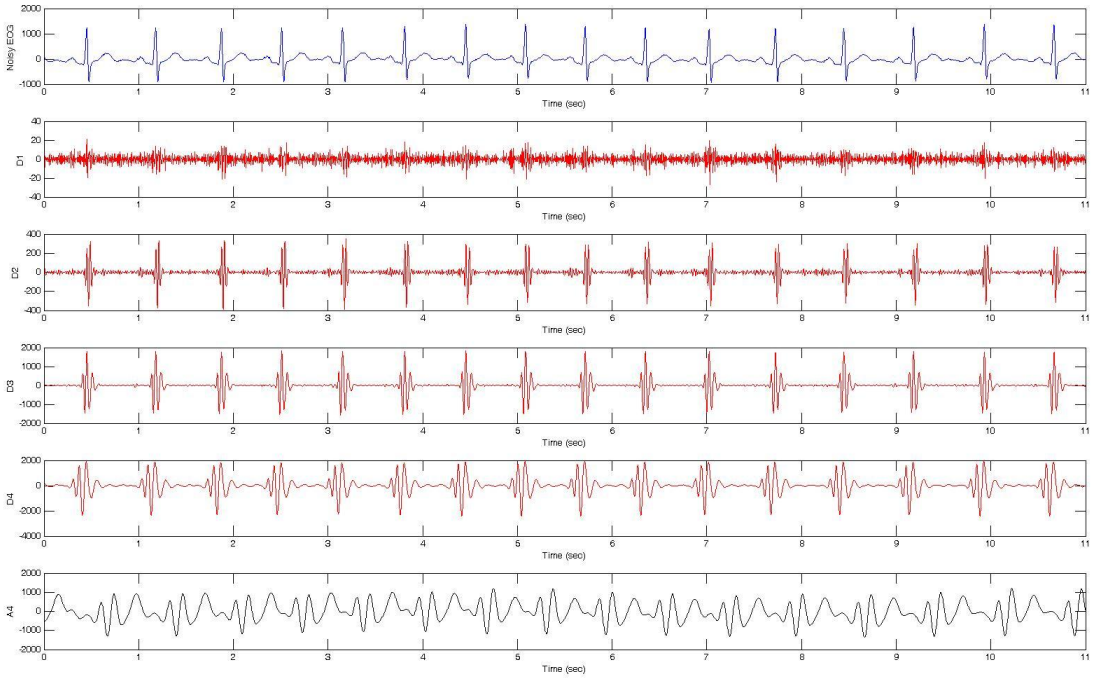

Figure 7 – Unfiltered detail and approximation coefficients for ECG signal

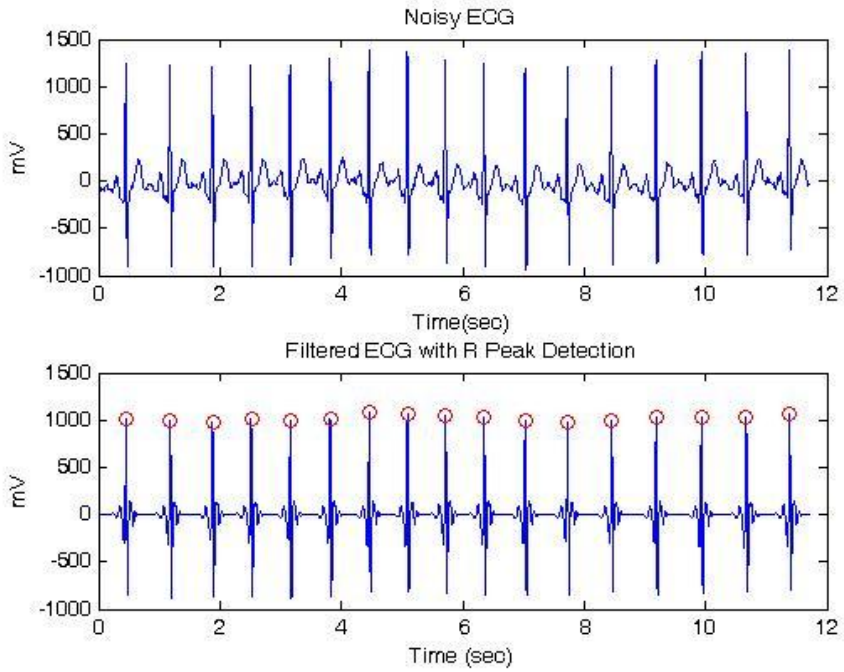

Figure 8 – real ECG (top) and filtered ECG with R-peak detection (bottom)

SCR:

The skin conductance response (SCR) is an important autonomic nervous system measure in physiological studies [11]. It's easily recorded, has a simple waveform, and its ability to indicate a response to a single stimuli [11].

Synthetic SCR:

In order to produce a synthetic SCR the four-parameter asymmetrical sigmoid-exponential will be used, this function is developed in [11]. The addition of Gaussian noise is made to a superimposed sequence of synthetic SCR signals to produce a realistic synthetic SCR. A comparison between the synthetic SCR and real SCR can be made in Figure 9.

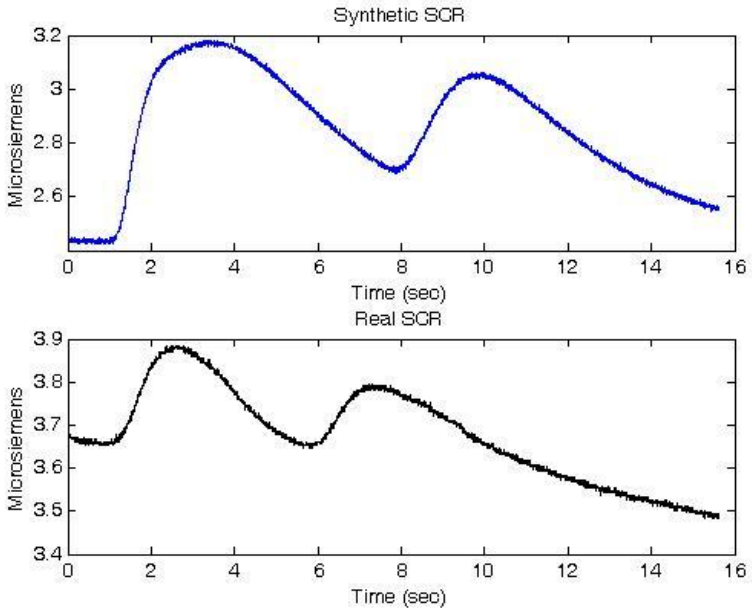

Figure 9 – Comparison between synthetic (top) and real SCR (bottom)

Filtering SCR:
The Daubechies-8 wavelet with an 8-level decomposition using Universal Threshold with the standard deviation for the Universal Threshold calculated using the MAD method. This method resulted in the best RMSE values when tested using the synthetic SCR waveforms, see Appendix A for details. The first 3 levels of the detail levels are set to zero because they do not contain any relevant data related to the SCR signal. A visual comparison between a filtered SCR and the noisy SCR can be made in Figure 10.

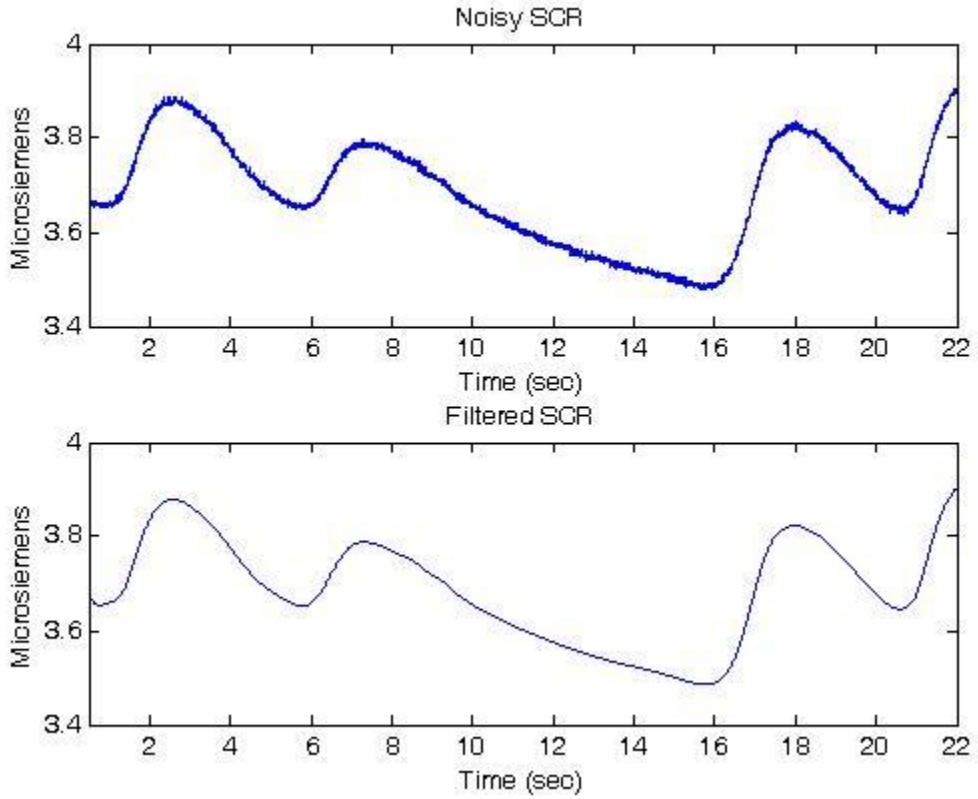

Figure 10 – Comparison between filtered (bottom) and noisy SCR (top)

B. Feature Extraction

After filtering the signals, a set of features were extracted from each physiological measure. Common used features were the normalized amplitude and normalized slope of the signal. In addition, an M-point moving average, a relative change with respect to the local mean, and an M-point moving standard deviation were considered. An M-point moving average smoothes out short-term fluctuations, captures longer-term trends an is defined as

$$x_{MovAvg}[n] = \frac{1}{M}\sum_{k=0}^{M-1} x[n-k].$$

The relative change with respect to the local mean can be expressed as

$$x_{rel}[n] = x[n] - x_{MovAvg}[n].$$

The M-point moving standard deviation measures the variability of a subset of the signal with respect to the local mean. This can be written as

$$x_{MovStd}[n] = \sqrt{\frac{1}{M}\sum_{i=0}^{M-1}\left(x[n-i] - x_{MovAvg}[n]\right)^2} \ .$$

Table I lists the chosen features for each signal. These were chosen by visually evaluating how these signals evolved when the robot was in motion

TABLE I
FEATURES EXTRACTED FROM SIGNALS

Physiological signal	Feature Extracted	Label
Skin Conductivity	Normalized Amplitude	SCR_{norm}
	Relative change with respect to local mean of normalized amplitude	SCR_{RelAvg}
	0.2 second moving standard deviation of normalized amplitude	SCR_{MovStd}
	0.2 second moving standard deviation of normalized slope	$dSCR_{MovStd}$
Electrocardiography	0.2-second moving average of normalized heart rate	HR_{norm}
	0.2 second moving standard deviation of normalized heart rate	HR_{MovStd}
	0.2 second moving standard deviation of normalized slope	dHR_{MovStd}
Electromyography	Normalized Amplitude	ENG_{norm}

C. Neural Network (NN)

In order to estimate the valence (the degree of how positive or negative an emotion is reported by the user, the Neural Network Toolbox from MATLAB was used. Neural networks are inspired by biological nervous systems [17]. The network is composed of simple elements, called neurons, operating in parallel to solve a specific problem. A neuron is a construct that takes many inputs and fires one output. Each element of the input is connected to each neuron input through a weight matrix. Training the network means to adjust the specific connecting weights so that a particular input leads to a specific target output [17]. Neural networks learn by example.

In this work, the input vector is a time-series signal containing a total of 8 features and 5900 elements (approximately 23 seconds). The training data were randomly divided as follows: 70% for training the NN, 15% for validation and 15% for testing. The target is the time-series valence reported by the participant. An additional time-series signal was used for further testing of the net containing 2500 elements.

Different numbers of neurons were used and the performance of the NN was compared. Additionally, several nets were trained their output averaged.

III. RESULTS

A linear regression plot can be used to evaluate the performance of the Neural Network. Figure 11 presents the linear regression between the output estimated by the NN and the target. It can be seen that for all Training, Validation and Testing, the R-value was over 0.99 and the response is satisfactory for the initial time-series input.

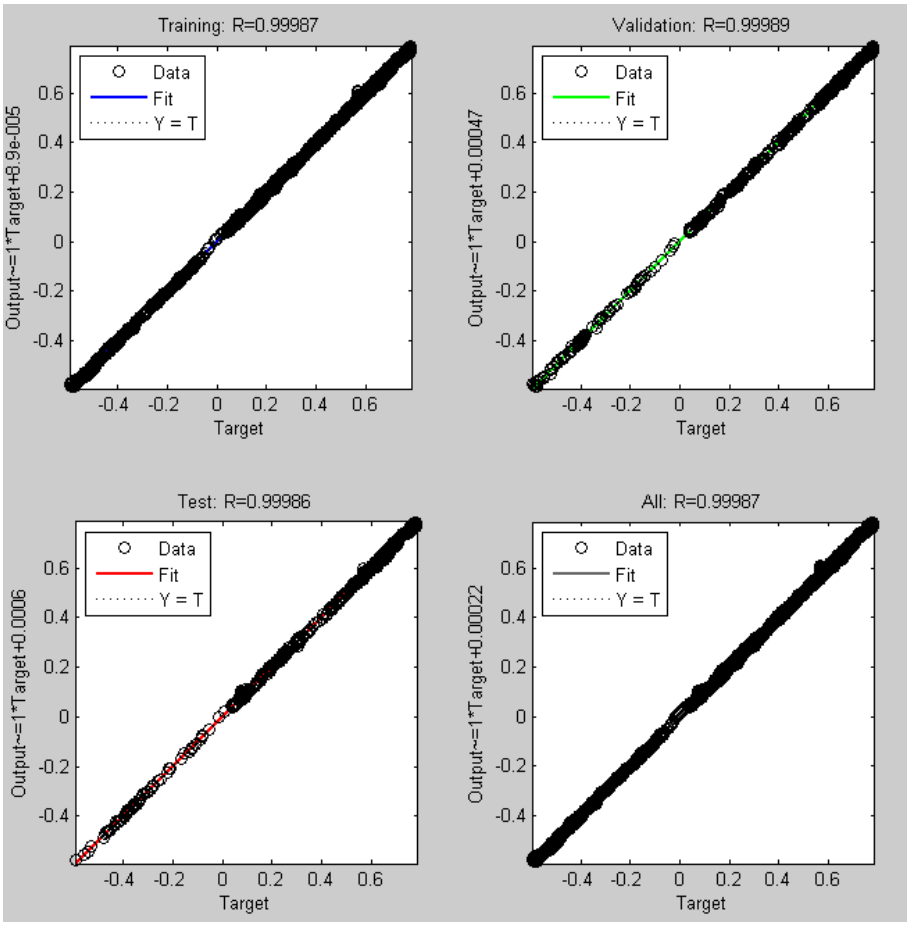

Figure 11 - Linear regression for Training, Validation and Testing of the NN

Figure 12 shows the valence estimated by the NN and the actual valence reported by the user. It can be observed that the NN was able to track the user response satisfactorily for the initial time-series used for training (70%), validation (15%) and testing (15%).

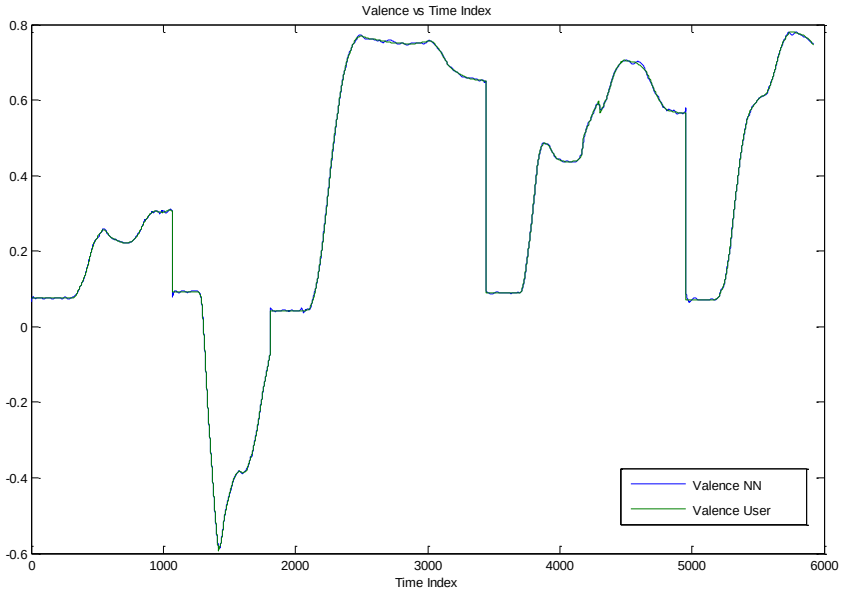

Figure 12 – Valence reported by user and estimated valence by NN for initial data set

Additionally, the mean absolute error was used to quantify the performance of the NN, that is how

much the estimated valence $x_{est}[n]$ deviates from the actual valence reported by the user $x_{act}[n]$.

$$MAE = \sum_{n=1}^{N} \left| x_{est}[n] - x_{act}[n] \right|.$$

The value of MAE was 0.023 for the initial time-series input.

In order to evaluate how the number of neurons and number of nets

Finally, Figure 13 plots the valence estimated by the NN and valence reported by the user for the additional data set. The response of the NN was not as satisfactory as desired and the *MAE* value was 0.31.

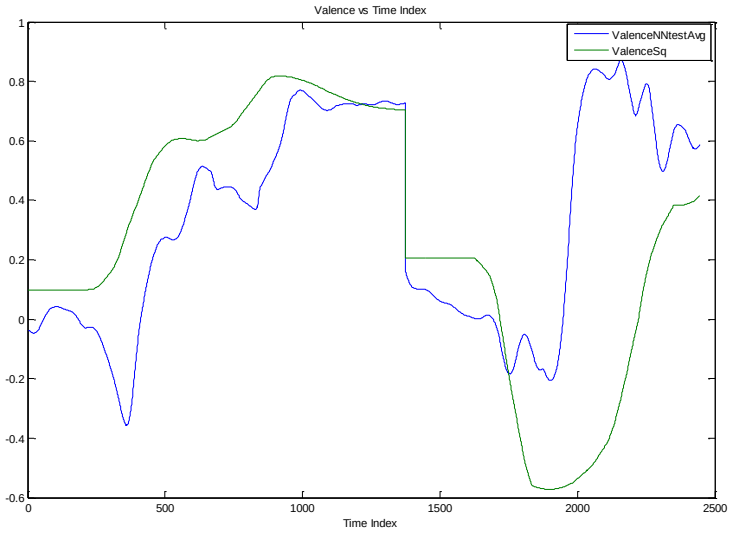

Figure 13 - Valence reported by user and estimated valence by NN for additional data set

IV. Discussions and Conclusions

In this report, we have implemented wavelet shrinkage techniques on electrocardiogram, electromyogram and skin conductance signals. There were some noise sources present that could not be removed using the following wavelet shrinkage methods. For the ECG a db8 wavelet was used with an 4-level decomposition using the Universal Threshold MAD and setting the first set of detail coefficients and approximation coefficients are set to zero. The EMG was filtered with a db1 with 7-level decomposition using SureShrink as the shrinkage method, as well the first level of decomposition coefficients are set to zero. The SCR was filtered using a db8 with a 7-level decomposition using Universal Threshold MAD as the shrinkage method; as well the first 3 levels of detail coefficients are set to zero.

In order to define some of these noise sources the collection of ECG, EMG, and SCR signals was done with known noise sources. These sources of noise include coughing, open-palmed chest compressions, heavy breathing, fast tapping of the sensor using fingers, twisting at the waist, standing, and clenching fist. Using this data a visual comparison from the acquired physiological signals with unknown noise and ones with known noise can be made.

ECG Noise Classification:

Figure 14 provides an example where it is clear that noise in the ECG signal is due to a compression from an object on the chest where the ECG electrode is placed.

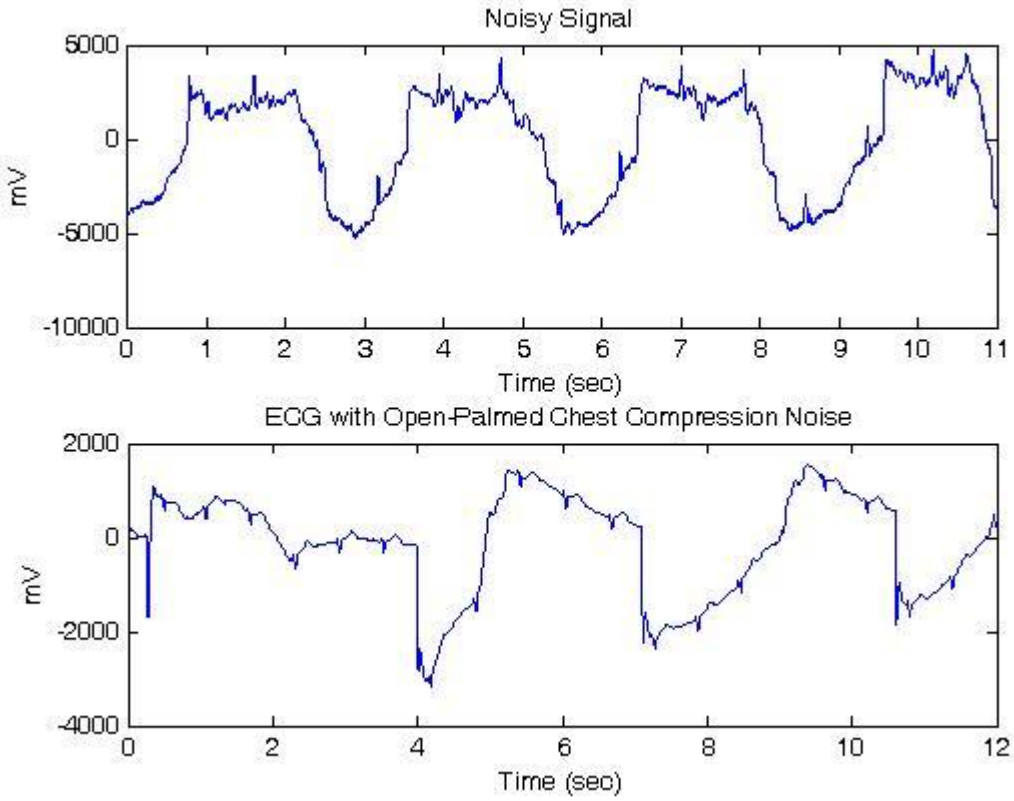

Figure 14 –ECG signal with noise due to a known source

Heavy breathing, hand clinching, and twisting are observed in all the ECG signals. This is expected because as the subjects ECGs are being recorded the subject must also squeeze and move a joystick while under different levels of stress. The artefacts of talking can be seen in the ECG but the effects cannot be seen if the single contains other muscle activity such as clenching the fist or twisting. None of the observed signals contained any noise resembling the noise produced from coughing.

EMG and SCR Noise Sources:

For the EMG signals there is no visual correlation between the noise events and any change in the EMG signals with unknown noise. This is also true for the SCR signals.

Neural Network performance:

Eight features were extracted from the filtered signals and fed into the neural network. The data set was divided into two batches. The first batch data were randomly divided for training, validation and testing. The second batch was used as additional testing to evaluate the network performance.

For the first batch, the neural network was able to successfully estimate the valence reported by the user with a mean absolute error of 0.023 and an R-correlation coefficient of 0.99 for testing data. For the second batch (additional testing data), the performance of the network was not as satisfactory as desired with a mean absolute error of 0.31. In order to improve these results, a more thorough analysis should be performed to select the best combination of features. Additionally, other physiological signals can be used, such as skin temperature, blood pressure, electroencephalography, etc. However, from the signal processing point of view, the wavelet shrinkage technique was proved useful for signal filtering.

V. References

[1] J. A. Russell, "A circumplex model of affect," Journal of Personality and Social Psychology, vol. 39, pp. 1161, 1980.
[2] "Thought Technology Ltd.," http://www.thoughttechnology.com
[3] Brani Vidakovic. Statistical Modeling by Wavelets. Canada: John Wiley & sons, 1999.
[4] Norman Allen Dyson and R. M. Smith. Chromatographic Integration Methods. Second Edition, Cambridge: The Royal Society of Chemistry, 1998.
[5] Adriano O. Andrade, Slawomir Nasuto, Peter Kyberd, Catherine M. Sweeney-Reed, F.R. Van Kanijn, EMG signal filtering based on Empirical Mode Decomposition, Biomedical Signal Processing and Control, Volume 1, Issue 1, January 2006, Pages 44-55, ISSN 1746-8094, DOI: 10.1016/j.bspc.2006.03.003.
http://www.sciencedirect.com/science/article/B7XMN-4K66FC7-1/2/d7a89c3dc03c0c85b6e3d0723e09212b
[6] Dimitrios Moshou, Ivo Hostens, G. P. & Ramon, H., Wavelets and self-organising maps in electromyogram (EMG) analysis 2000
http://www.erudit.de/erudit/events/esit2000/proceedings/AE-01-4-P.pdf
[7] Martha Flanders, Choosing a wavelet for single-trial EMG, Journal of Neuroscience Methods, Volume 116, Issue 2, 15 May 2002, Pages 165-177, ISSN 0165-0270, DOI: 10.1016/S0165-0270(02)00038-9.
http://www.sciencedirect.com/science/article/B6T04-45H98TN-1/2/eb29dc406d2f54175d1b07f4be8cac84
[8] Merlo, A.; Farina, D.; Merletti, R., "A fast and reliable technique for muscle activity detection from surface EMG signals," Biomedical Engineering, IEEE Transactions on , vol.50, no.3, pp.316-323, March 2003
http://ieeexplore.ieee.org/stamp/stamp.jsp?arnumber=1186735&isnumber=26615
[9] McSharry, P.E.; Clifford, G.D.; Tarassenko, L.; Smith, L.A., "A dynamical model for generating synthetic electrocardiogram signals," Biomedical Engineering, IEEE Transactions on , vol.50, no.3, pp.289-294, March 2003
http://ieeexplore.ieee.org/stamp/stamp.jsp?arnumber=1186732&isnumber=26615
[10] Brij N. Singh, Arvind K. Tiwari, Optimal selection of wavelet basis function applied to ECG signal denoising, Digital Signal Processing, Volume 16, Issue 3, May 2006, Pages 275-287, ISSN 1051-2004, DOI: 10.1016/j.dsp.2005.12.003.
http://www.sciencedirect.com/science/article/B6WDJ-4J4HJ6X-1/2/cad695db5ece60cd9b760fc23ee76790
[11] Chong L. Lim, Chris Rennie, Robert J. Barry, Homayoun Bahramali, Ilario Lazzaro, Barry Manor, Evian Gordon, Decomposing skin conductance into tonic and phasic components, International Journal of Psychophysiology, Volume 25, Issue 2, February 1997, Pages 97-109, ISSN 0167-8760, DOI: 10.1016/S0167-8760(96)
00713-1.
http://www.sciencedirect.com/science/article/B6T3M-4BJN36M-2/2/641a81dfa4510ffad5dd579e6398254f
[12] Sandro A. P. Haddad and Wouter A. Serdijn. Ultra Low-Power Biomedical Signal Processing. Netherlands: Springer Netherlands, 2009
http://www.springerlink.com/content/n3200557v2087058/
[13] Hernandez-Fajardo, Isaac, Georgios Evangelatos, Ioannis Kougioumtzoglou, and Xin Ming. Signal Denoising using Wavelet-based Methods. Connexions. 16 Dec. 2008
http://cnx.org/content/m18931/1.2/
[14] S. Poornachandra, Wavelet-based denoising using subband dependent threshold for ECG signals, Digital Signal Processing, Volume 18, Issue 1, January 2008, Pages 49-55, ISSN 1051-2004, DOI: 10.1016/j.dsp.2007.09.006.
http://www.sciencedirect.com/science/article/B6WDJ-4PRRBMN-2/2/5950f41c0609f8342e454e3df0dc427d
[15] Prasad, V.V.K.D.V.; Siddaiah, P.; Rao, B.P., "Denoising of Biological Signals using a New Wavelet Shrinkage Method," Industrial and Information Systems, 2008. ICIIS 2008. IEEE Region 10 and the Third international Conference on , vol., no., pp.1-5, 8-10 Dec. 2008
http://ieeexplore.ieee.org/stamp/stamp.jsp?arnumber=4798410&isnumber=4798312
[17] Matlab V6.0.2 (R2009a) Neural Network Toolbox.

Appendix A:
Analysis of RMSE values given different wavelet shrinkage techniques

SCR Wavelet Filter Analysis

	db1	db2	db3	db4	db5	db6	db7	db8
UnivST	0.336112	0.319358	0.318185	0.316086	0.315879	0.315668	0.314931	0.314598
UnivMAD	0.344784	0.326223	0.323515	0.322785	0.322747	0.32149	0.322372	0.322429
CV	0.596225	0.596225	0.596225	0.596225	0.596225	0.596225	0.596225	0.596225
SS	2.493222	1.804985	1.691774	1.659069	1.648761	1.646603	1.647801	1.650445
BJ	0.786806	0.823852	0.772734	0.773076	0.825546	0.827117	0.792106	0.809213

RMSE: 0.3146

Wavelet: db8

Wavelet Filter: UnivMAD

EMG Wavelet Filter Analysis

	db1	db2	db3	db4	db5	db6	db7	db8
UnivR	93.88776	95.76369	96.16104	96.38023	96.3778	96.52559	96.47994	96.42397
UnivMAD	96.42467	97.29361	97.45778	97.61965	97.60823	97.74927	97.70767	97.68206
CV	140.0138	140.0138	140.0138	140.0138	140.0138	140.0138	140.0138	140.0138
SS	84.13212	89.36467	90.84722	91.54518	91.96065	92.24324	92.45203	92.61488
BJ	139.6824	139.6823	139.6893	139.6905	139.6766	139.6828	139.6988	139.7115

RMSE: 84.1321

Wavelet: db1

Wavelet Filter: SS

ECG Wavelet Filter Analysis

	db1	db2	db3	db4	db5	db6	db7	db8
UnivR	4.598995	4.578944	4.574496	4.574399	4.573541	4.574508	4.573612	4.569769
UnivMAD	4.637259	4.577715	4.573195	4.573973	4.574185	4.574058	4.573055	4.569837
CV	4.650391	4.647972	4.650391	4.650391	4.650391	4.650391	4.650391	4.650391
SS	7.218552	7.280538	7.806748	7.292144	7.654115	8.177051	8.933452	8.85549
BJ	4.5752	4.617434	4.610899	4.596825	4.632705	4.587409	4.578481	4.590879

RMSE: 4.5698

Wavelet: db8

Wavelet Filter: UnivMAD